



Published in final edited form as:

Cell Rep. 2018 February 20; 22(8): 2190–2205. doi:10.1016/j.celrep.2018.01.087.

A Roadmap for Human Liver Differentiation from Pluripotent Stem Cells

Lay Teng Ang^{1,12}, Antson Kiat Yee Tan^{1,10}, Matias I. Autio^{2,3,10}, Su Hua Goh¹, Siew Hua Choo¹, Kian Leong Lee⁴, Jianmin Tan¹, Bangfen Pan^{2,3}, Jane Jia Hui Lee^{1,5}, Jen Jen Lum^{1,6}, Christina Ying Yan Lim¹, Isabelle Kai Xin Yeo^{1,6}, Chloe Jin Yee Wong^{1,6}, Min Liu⁸, Jueween Ling Li Oh^{1,6}, Cheryl Pei Lynn Chia^{1,6}, Chet Hong Loh¹, Angela Chen⁷, Qingfeng Chen^{8,9}, Irving L. Weissman⁷, Kyle M. Loh^{7,11}, and Bing Lim^{1,11}

¹Stem Cell & Regenerative Biology Group, Genome Institute of Singapore, A*STAR, Singapore 138672, Singapore

²Human Genetics Group, Genome Institute of Singapore, A*STAR, Singapore 138672, Singapore

³Cardiovascular Research Institute, National University of Singapore, Singapore 117599, Singapore

⁴Cancer and Stem Cell Biology Program, Duke-NUS Medical School, Singapore 169857, Singapore

⁵School of Biological Sciences, Nanyang Technological University, Singapore 637551, Singapore

⁶School of Engineering, Temasek Polytechnic, Singapore 529757, Singapore

⁷Stanford Institute for Stem Cell Biology & Regenerative Medicine, Department of Developmental Biology, Stanford-UC Berkeley Siebel Stem Cell Institute, Stanford University School of Medicine, Stanford, CA 94305, USA

⁸Humanized Mouse Unit, Institute of Molecular and Cell Biology, A*STAR, Singapore 138673, Singapore

⁹Department of Microbiology, Yong Yoo Lin School of Medicine, National University of Singapore, Singapore 119228, Singapore

Summary

This is an open access article under the CC BY-NC-ND license (<http://creativecommons.org/licenses/by-nc-nd/4.0/>).

Correspondence to: Lay Teng Ang; Bing Lim.

¹⁰These authors contributed equally

¹¹Senior author

¹²Lead Contact

Supplemental Information: Supplemental Information includes Supplemental Experimental Procedures, six figures, and five tables and can be found with this article online at <https://doi.org/10.1016/j.celrep.2018.01.087>.

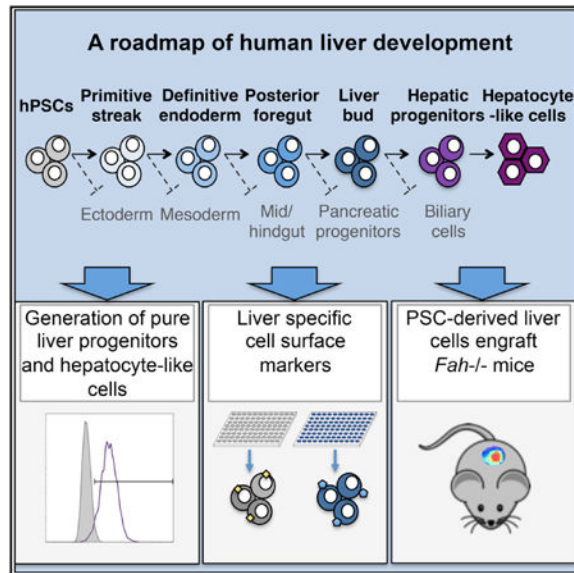
Author Contributions: L.T.A. designed the experiments. L.T.A., A.K.Y.T., S.H.G., S.H.C., J.T., and C.H.L. differentiated hPSCs and, with Q.F.C., J.J.H.L., and M.L., transplanted hPSC-derived hepatocytes. M.I.A. performed western blotting and generated the reporter line with B.P. K.L.L. generated and analyzed microarray data. J.J.L., C.Y.Y.L., K.X.Y., J.Y.W., L.L.O., and P.L.C. performed molecular characterization of differentiated hPSCs. K.M.L., A.C., and I.L.W. conducted surface marker analyses. L.T.A., K.M.L., and B.L. oversaw the study and wrote the manuscript.

Declaration of Interests: The authors declare that they have a patent (PCT/SG2015/050381) related to this work.

How are closely related lineages, including liver, pancreas, and intestines, diversified from a common endodermal origin? Here, we apply principles learned from developmental biology to rapidly reconstitute liver progenitors from human pluripotent stem cells (hPSCs). Mapping the formation of multiple endodermal lineages revealed how alternate endodermal fates (e.g., pancreas and intestines) are restricted during liver commitment. Human liver fate was encoded by combinations of inductive and repressive extracellular signals at different doses. However, these signaling combinations were temporally re-interpreted: cellular competence to respond to retinoid, WNT, TGF- β , and other signals sharply changed within 24 hr. Consequently, temporally dynamic manipulation of extracellular signals was imperative to suppress the production of unwanted cell fates across six consecutive developmental junctures. This efficiently generated 94.1% \pm 7.35% TBX3⁺ HNF4A⁺ human liver bud progenitors and 81.5% \pm 3.2% FAH⁺ hepatocyte-like cells by days 6 and 18 of hPSC differentiation, respectively; the latter improved short-term survival in the *Fah*^{-/-} *Rag2*^{-/-} *Il2rg*^{-/-} mouse model of liver failure.

Graphical abstract

Ang et al. chart how human liver progenitors develop from pluripotent stem cells through six developmental steps, including extracellular signals and surface markers associated with liver formation. This knowledge enables efficient generation of liver bud progenitors and, subsequently, hepatocyte-like cells that could function *in vivo* and *in vitro*.



Introduction

A quintessential goal of developmental biology is to understand how stem cells and progenitors commit to a singular lineage among multiple alternate fate choices (Graf and Enver, 2009). For instance, multiple lineages including liver, pancreas, and intestines emanate from a common progenitor. Paradoxically, the formation of these lineages has been ascribed to a common set of signals (e.g., bone morphogenetic protein [BMP] and/or fibroblast growth factor [FGF]) based on pioneering genetic knockouts that demonstrated

that these signals are broadly necessary for the development of each of these lineages *in vivo* (Bhushan et al., 2001; Chung et al., 2008; Jung et al., 1999; Rossi et al., 2001; Shin et al., 2007). This raises the question of how these lineages are diversified from one another. Often, we do not understand cell-type specification at a level of granularity to know what precise combinations of signals specify cell fate at any given time (Wandzioch and Zaret, 2009). However the differentiation of pluripotent stem cells (PSCs; including embryonic and induced pluripotent stem cells) provides a reductionist system to reveal the minimal extracellular signals sufficient for specifying a given cell type from scratch. Hence, analogous to embryonic explant cultures (Gualdi et al., 1996; Serls et al., 2005), PSC differentiation might allow us to uncover the combinations and timings of signals that specify cell fate at a level of detail difficult to achieve *in vivo*. Here, we took the latter approach to better understand liver development; we demonstrate that liver commitment is executed by signals that exclude alternate lineage options in stepwise fashion across six consecutive lineage choices.

Pluripotent cells develop into liver cells through multiple consecutive branching lineage choices, which have been partially delineated through studies of early vertebrate embryos (Duncan, 2003; Gordillo et al., 2015; Lemaigre, 2009; Lewis and Tam, 2006; Miyajima et al., 2014) but remain to be fully elucidated. In the early mouse embryo, the pluripotent epiblast (at embryonic day 5.5 [\sim E5.5]) differentiates into the anterior primitive streak (\sim E6.5) and, subsequently, the definitive endoderm germ layer (\sim E7–E7.5) (Lawson et al., 1991; Tam and Beddington, 1987). Definitive endoderm is the common progenitor to epithelial cells in diverse internal organs, including the liver, pancreas, and intestines (Spence et al., 2009; Tremblay and Zaret, 2005) (Figure 1A).

Shortly thereafter, by \sim E8.5, endoderm is patterned along the anterior-posterior axis to broadly form the anterior foregut, posterior foregut, and midgut/hindgut (Grapin-Botton, 2005; Zorn and Wells, 2009). By \sim E9.5, the posterior foregut gives rise to either pancreatic progenitors or the earliest liver progenitors—known as liver bud progenitors (Fukuda-Taira, 1981; Ledouarin, 1964; Rossi et al., 2001)—as shown by single-cell lineage tracing (Chung et al., 2008). Conversely, the midgut/hindgut gives rise to intestinal epithelium (Spence et al., 2011a). Subsequently, incipient \sim E9.5 liver bud progenitors are thought to differentiate over the course of several days into either hepatocytes or bile duct cells (cholangiocytes)—the two major epithelial constituents of the liver (Suzuki et al., 2008b). At birth, early hepatocytes already express characteristic genes (e.g., *Albumin*, *Cps1*, and *Fah*) (Cascio and Zaret, 1991; Chen et al., 2009) but diversify to form multiple functionally distinct hepatocyte subsets after birth (Colnot and Perret, 2011; Jungermann, 1995; Shiojiri et al., 1995; Spijkers et al., 2001), including periportal or pericentral hepatocytes that encircle, respectively, either portal or central veins (Smith and Campbell, 1988).

There has been major headway in reconstituting enriched populations of hepatocyte-like cells from human PSCs (hPSCs) (Agarwal et al., 2008; Basma et al., 2009; Cai et al., 2007; Carpentier et al., 2014, 2016; Espejel et al., 2010; Han et al., 2012; Ogawa et al., 2013; Rashid et al., 2010; Si-Tayeb et al., 2010; Song et al., 2009; Touboul et al., 2010; Zhao et al., 2013). Put simply, the prevailing view is that, in order to generate hepatocyte-like cells from hPSCs, liver development should be divided into roughly three stages over several weeks or

months. Current protocols to differentiate hPSCs toward liver generally commence with (1) ACTIVIN/transforming growth factor β (TGF- β (in the presence or absence of WNT) to initially induce endoderm; followed by (2) BMP and FGF to specify liver progenitors; and, finally, (3) hepatocyte growth factor (HGF), Oncostatin M (OSM), dexamethasone, and/or 3D reaggregation with other cell types to specify hepatocytes (Cai et al., 2007; Carpentier et al., 2014; Gouon-Evans et al., 2006; Ogawa et al., 2013; Rashid et al., 2010; Si-Tayeb et al., 2010; Song et al., 2009; Takebe et al., 2013; Touboul et al., 2010; Zhao et al., 2013). However, current three-step differentiation approaches may not precisely mirror liver development, as liver development from pluripotent cells *in vivo* likely entails more than three steps. Indeed, certain differentiation protocols generate impure populations containing a subset of hPSC-derived liver cells; upon transplantation, these impure populations yielded tumors (Haridass et al., 2009).

Here, we reconstitute early liver development through a sequence of six consecutive lineage choices and detail the signals at each juncture that specify each cell type (either liver or non-liver lineages). This map of liver development allowed us to more precisely control differentiation: by mapping the generation of closely related endodermal lineages (liver, pancreatic, and midgut/hindgut progenitors), we developed a strategy to exclusively specify liver progenitors while suppressing formation of unwanted lineages (i.e., pancreas and midgut/hindgut). Strikingly, we also showed that multiple developmental signals (e.g., retinoid, TGF- β , Wnt, and other signals) have opposing effects within 24 hr, initially specifying one fate and then subsequently repressing its formation. The temporally dynamic action of these signals contrasts with how these signals are typically added for multiple days in some prevailing differentiation schema. Hence, manipulating signals in a temporally dynamic fashion enabled the faster production of $94.1 \pm 7.35\%$ HNF4A⁺ liver bud progenitors from hPSCs within 6 days. Importantly, the hPSC-derived liver bud progenitors produced could further differentiate into $81.5 \pm 3.2\%$ FAH⁺ hepatocyte-like cells, the latter of which could function *in vitro* and improve short-term survival in the *Fah*^{-/-}*Rag2*^{-/-}*Ilr2g*^{-/-} (FRG) mouse model of liver injury.

Finally, we furnish tools to quantitatively track this liver differentiation process. These include cell-surface markers identifying liver progenitors (which we find to be CD99⁺CD184⁻CD10⁻) and a knockin reporter hPSC line to track the expression of metabolic enzyme *FAH* during hepatocyte differentiation.

Results

RA, BMP, and FGF Activation and TGF- β Inhibition Differentiate Endoderm into Posterior Foregut with the Competence to Later Generate Liver Bud Progenitors

Pluripotent cells first differentiate into primitive streak and, subsequently, definitive endoderm before turning into liver (Figure 1A). We previously identified signals to differentiate hPSCs into >99% pure MIXL1-GFP⁺ primitive streak cells in 24 hr (Figures 1B and 1C) and, subsequently, into >98% pure SOX17-mCherry⁺ definitive endoderm by day 2 of differentiation (Figures 1B and 1D) (Loh et al., 2014, 2016). These nearly pure day-2 endoderm populations, whose purity has been corroborated by other groups (Rostovskaya et al., 2015), provided an optimal starting point to examine signals that could further generate

day-3 posterior foregut and, later, day-6 liver bud progenitors (Figure 1F). Since *Tbx3*, *Afp*, *Prox1*, *Cebpa*, *Hnf4a*, *Hnf6*, and *Hnf1b* (Jacquemin et al., 2003; Lokmane et al., 2008; Lüdtke et al., 2009; Shiojiri et al., 2004; Suzuki et al., 2008a) are expressed in E9.5 mouse liver bud progenitors (Figure 1E), their human homologs were used as markers to assess the generation of hPSC-derived liver bud progenitors.

Current efforts to differentiate hPSC-derived endoderm into liver progenitors often continuously apply the same signals for several days (Carpentier et al., 2016; Si-Tayeb et al., 2010); by contrast, we found that two opposing groups of signals specified posterior foregut and, subsequently, liver bud progenitors. First, we determined that transient activation of the retinoic acid (RA), BMP, and FGF pathways together with inhibition of TGF- β signaling for 24 hr was critical to differentiate day-2 definitive endoderm into day-3 posterior foregut that was competent to later differentiate into liver bud progenitors.

RA agonists initially promoted posterior foregut specification on day 3 of differentiation. Treatment of day-2 endoderm with the RA agonists all-*trans* RA (ATRA; 2 μ M) or 4-[(*E*)-2-(5,6, 7,8-Tetrahydro-5,5,8,8-tetramethyl-2-naphthalenyl)-1-propenyl] benzoic acid (TTNPB) (75 nM) for 24 hr enhanced the formation of day-3 posterior foregut that was later competent to differentiate into liver bud (Figures 1F–1H) and downstream hepatocytes (Figures S1A and S1B) on later days of differentiation. Thus, RA is crucial for human posterior foregut specification, consistent with the role for RA in generating foregut derivatives such as stomach endoderm *in vitro* (McCracken et al., 2014) and how inhibiting RA synthesis abrogates both liver and pancreas formation in zebrafish embryos (Stafford and Prince, 2002).

Foregut specification by day 3 was also promoted by TGF- β inhibition (Figure 1I) and activation of the BMP (Figure 1J) and FGF pathways (Figures S1D and S1E). Unexpectedly, although BMP inhibition expanded the foregut domain in *Xenopus* and zebrafish (Rankin et al., 2011; Tiso et al., 2002), conversely, day-3 BMP inhibition reduced the competence of hPSC-derived foregut progenitors to later differentiate into liver bud progenitors (Figure 1J). Each of these 24-hr manipulations to initially generate foregut had far-reaching effects and enhanced the generation of posterior foregut that was capable of subsequently differentiating into liver bud progenitors and hepatocytes (Figures 1H–1J and S1A–S1C).

Taken together, day-2 definitive endoderm could be converted into day-3 posterior foregut by the simultaneous activation of RA, BMP, and FGF pathways together with inhibition of TGF- β signaling for 24 hr. Such day-3 hPSC-derived posterior foregut expressed *HHEX* (Figure S1H), a marker of ~E8.5 mouse ventral posterior foregut (Thomas et al., 1998).

TGF- β , BMP, and PKA Activation and WNT Inhibition Induce Differentiation of Foregut into Liver Bud Progenitors by Day 6 of Differentiation

Subsequent progression of day-3 hPSC-derived posterior foregut into day-6 liver bud progenitors required distinct signals (Figure 2A). Although day-3 posterior foregut was initially specified by RA activation and TGF- β inhibition, the subsequent differentiation of posterior foregut into day-6 liver bud progenitors was suppressed by continued RA activation and TGF- β inhibition. This highlights the temporally dynamic action of these

signals. Instead, liver bud specification on days 4–6 required activation of the TGF- β , BMP, and protein kinase A (PKA) pathways, together with WNT inhibition, for 48–72 hr (Figure 2B).

While RA initially differentiated endoderm into day-3 posterior foregut (discussed earlier), 24 hr later, it repressed subsequent progression into liver bud progenitors and promoted formation of *ODD1*⁺ stomach endoderm on days 4–6 (Figure 2C). Hence, our findings reconcile conflicting findings that RA is, overall, required for zebrafish liver induction (Stafford and Prince, 2002) but that RA-coupled beads inhibit liver bud marker formation in Hamburger Hamilton Stage 10 (HH10)-stage zebrafish embryos (Bayha et al., 2009); there is a temporally dynamic requirement for RA in liver bud specification.

Akin to RA signaling, the role for TGF- β in liver specification was also temporally dynamic: TGF- β *inhibition* initially promoted foregut formation by day 3 (Figure 1I), but 24 hr later, TGF- β *activation* promoted liver bud specification on days 4–6, leading to enhanced liver bud marker expression by day 6 (Figure 2D). Emphasizing the importance of TGF- β activation, we found that TGF- β inhibition at this stage abrogated the differentiation of foregut into liver bud (Figure 2D), contrasting with earlier use of TGF- β inhibitors to differentiate hPSC-derived endoderm into liver (Loh et al., 2014; Sampaziotis et al., 2015; Touboul et al., 2010).

BMP and PKA activation, together with WNT blockade, also cooperated with TGF- β activation to differentiate day-3 foregut into day-6 liver bud progenitors. Consistent with earlier findings (Chung et al., 2008; Rossi et al., 2001; Shin et al., 2007; Si-Tayeb et al., 2010; Wandzioch and Zaret, 2009; Zhao et al., 2013), first, we found that BMP or FGF activation differentiated foregut into liver bud while blocking pancreas formation (Figures 2E, S2D, and S2E); by contrast, BMP or FGF inhibition suppressed liver formation (Figures 2E, S2D, and S2E). This mirrors how *bmp2b* overexpression promotes liver specification at the expense of pancreatic progenitors in zebrafish embryos (Chung et al., 2008) and how BMP induces liver from mouse embryonic endoderm explants (Rossi et al., 2001). Second, we found that PKA agonists (e.g., 8-bromo-cAMP) also potently specified liver bud from foregut (Figure 2F), supporting the notion that prostaglandin E2 specifies zebrafish liver progenitors by activating the PKA cascade (Nissim et al., 2014). Finally, WNT inhibition (using C59) from days 4 to 5 suppressed midgut/hindgut (MHG; posterior endoderm) formation (Figures S1F and S1G) and, instead, transiently promoted the formation of liver bud progenitors that had the ability to subsequently form hepatocytes (Figures S2B and S2C). This is consistent with how WNT blocks foregut formation and, instead, specifies midgut/hindgut in *Xenopus* (McLin et al., 2007) but subsequently promotes proliferation of liver progenitors (Sekine et al., 2006). In summary, we showed that simultaneous activation of TGF- β , BMP, and PKA—but transient suppression of WNT—drove day-3 posterior foregut into day-6 liver bud progenitors while simultaneously blocking pancreatic and midgut/hindgut differentiation.

This approach rapidly generated an 85.8%, a 92%, and an 89.2% pure AFP⁺ liver bud progenitor population by day 6 of differentiation from the H1, H7, and H9 hPSC lines, respectively (Figures 2G and 2H). Day-6 liver bud progenitors expressed liver bud

transcription factors *HNF4A*, *TBX3*, *HNF6*, and *CEBPA*, which were low or undetectable in midgut/hindgut (Figures 2C – 2F and S2A). Reciprocally, hPSC-derived liver bud progenitors did not express *CDX* or *HOX* genes (Figures 2I and S2A), which are markers of the midgut/hindgut, a developmentally related lineage that emanates from adjacent posterior endoderm and is also specified by BMP and FGF signals (Sherwood et al., 2011; Spence et al., 2011b). Dorsal (*MNX1*), stomach (*ODD1*), and pancreatic (*PDX1*) endoderm markers were low or undetectable in hPSC-derived liver bud progenitors in comparison to hPSC-derived pancreatic endoderm or midgut/hindgut (Figure 2I).

Taken together, though liver bud and midgut/hindgut (intestinal) progenitors are spatially adjacent *in vivo*, they are transcriptionally distinct lineages and can be produced in mutually exclusive signaling conditions *in vitro* from hPSCs. Importantly, while there is a common requirement for BMP and FGF in liver and midgut/hindgut specification, we revealed signals that uniquely specify liver, thus clarifying how these lineages become segregated from one another.

Finally, this PSC-to-liver bud differentiation system was significantly more rapid and yielded higher expression of liver bud markers, compared to four extant liver differentiation methods (Avior et al., 2015; Carpentier et al., 2016; Chen et al., 2012; Si-Tayeb et al., 2010; Zhao et al., 2013) (Figures 3A–3C and S3C). By day 6 of hPSC differentiation, 94.1% \pm 7.35% HNF4A⁺ pure liver bud progenitors were produced (Figure S3A), whereas HNF4A⁺ liver progenitors were typically formed on later days (by day 10–14) in other differentiation protocols (Carpentier et al., 2016; Hay et al., 2008; Si-Tayeb et al., 2010; Zhao et al., 2013). Hence the temporally dynamic manipulation of extracellular signals enables the efficient generation of human liver bud progenitors by day 6 of PSC differentiation, which is \sim 2 times faster than extant methods.

A Surface Marker Signature for hPSC-Derived Liver Bud Progenitors

To quantitatively track the time course of human liver bud progenitor specification at the single-cell level, we next sought to identify lineage-specific cell-surface markers for day-0 hPSCs, day-2 definitive endoderm, and day-6 liver bud progenitors. Systematically screening the expression of 242 cell-surface antigens on these 3 lineages revealed stage-specific surface markers (Figures 3C and 3D). First, CD10 was expressed in 92.6 \pm 5.6% of undifferentiated hPSCs but was abruptly down-regulated upon differentiation, being expressed in <2% of cells in day-2 definitive endoderm or day-6 liver bud populations (Figures 3E and S3B; Table S1). Second, CD184/CXCR4 (a known definitive endoderm marker; D'Amour et al., 2005) was enriched in day-2 definitive endoderm in comparison to day-0 hPSCs and day-6 liver bud progenitors (Figure 3E; Table S1). Finally, CD99 was highly expressed on day-6 liver bud progenitors by comparison to preceding hPSCs or definitive endoderm (DE) (Figures 3C and 3D; Table S1). This pattern was consistent across a panel of 4 hPSC lines (H7, HES2, H1, and BJC1; Figure S3B; Table S1). Thus, a CD99^{hi}CD10⁻CD184^{lo/-} surface marker profile may be used to track the early specification of, and enrich for, hPSC-derived liver bud progenitors (Figure 3F).

Segregation of Human Liver Bud Progenitors into Hepatocyte versus Biliary Fates by Competing NOTCH, TGF- β , PKA, and Other Signals

Next, we identified signals that induced the bifurcation of hPSC-derived day-6 liver bud progenitors into *ALBUMIN*⁺ hepatocyte-like cells or *SOX9*⁺ biliary cells (cholangiocytes) (Figures 4A and 4B) on later days of differentiation. Activation of NOTCH and TGF- β , together with insulin, upregulated *SOX9*, thus differentiating day-6 liver bud progenitors into CK7⁺/CK19⁺ biliary progenitors by day 12 of hPSC differentiation (Figures 4B and S4H) (Ogawa et al., 2015; Sampaziotis et al., 2015) while reducing formation of *ALBUMIN*⁺ hepatocyte-like cells (Figures 4C and 4D). Conversely, inhibition of NOTCH and TGF- β consolidated hepatocyte commitment by inhibiting diversion into the *SOX9*⁺ biliary fate (Figures 4C and 4D). This suggests the bipotent capacity of liver bud progenitors at a population level to give rise to either hepatic or biliary fates (which remains to be formally demonstrated *in vivo* by single-cell lineage tracing) and identifies the signals that control the mutually exclusive allocation of *ALBUMIN*⁺ hepatocyte-like versus *SOX9*⁺ cholangiocyte lineages.

Beyond expression of pan-hepatocyte marker *ALBUMIN*, we sought to identify signals that would upregulate the expression of various metabolic enzymes in hPSC-derived hepatocytes. This is important because hPSC-derived hepatocytes are often less metabolically functional than primary human hepatocytes (Camp et al., 2017; Carpentier et al., 2016). In particular, we sought to promote expression of tyrosine metabolism pathway components, as genetic deficiency of tyrosine metabolic enzymes (e.g., *fumarylacetoacetate hydrolase [FAH]*) results in hereditary tyrosinemia in human patients, a metabolic disorder (St-Louis and Tanguay, 1997). High insulin levels, together with a stabilized ascorbic acid derivative (ascorbic acid-2-phosphate [AAP]) greatly promoted the expression of tyrosine metabolic pathway genes *PAH*, *HGD*, *HPD*, *TAT*, *MAI*, and *FAH* and other liver markers by 18 days of differentiation (Figures S4C and S4F). PKA agonists (e.g., 8-bromo-cAMP and forskolin) also had a similar effect (Figure S4D). Microarray profiling showed that treatment with NOTCH inhibitor, AAP, forskolin, or insulin upregulated genes associated with gene ontology classifications pertaining to metabolic processes (Figures 4F and S4I; Table S5), asserting that these individual manipulations each promote the metabolic competence of hPSC-derived hepatocytes.

Combining these signals efficiently generated *ALBUMIN*⁺ hepatocyte-like cells by day 18 of differentiation, which displayed various hepatocyte functions *in vitro*. First, provision of the aforementioned hepatocyte-specifying signals, together with transient inhibition of cholangiocyte-specifying signals TGF- β and NOTCH, yielded 88.7%, 77.3%, and 95.9% pure *ALBUMIN*⁺ hepatocyte-like cells from the H1, H7, and H9 hPSC lines, respectively (Figures 4E and S4K), as assessed by intracellular flow cytometry after 18 days of hPSC differentiation. Second, day-18 hPSC-derived hepatocytes secreted *ALBUMIN* and *FIBRINOGEN* proteins into the medium (5.89 ± 0.71 $\mu\text{g/mL}$ and 1.38 ± 0.26 $\mu\text{g/mL}$, respectively [Figures 4G and S4L]) in the same order of magnitude as the amount secreted by hepatocytes *in vivo* in human beings (Bernardi et al., 2012; Tennent et al., 2007). Third, hPSC-derived hepatocyte-like cells possessed CYP3A4 enzymatic activity at levels 5.9-fold higher than those of HepG2 cells, although they were still 55-fold lower than in primary

adult human hepatocytes (Figure 4H). Fourth, they stained positive for periodic acid Schiff (implying glycogen storage; Figure S4M) as well as the liver-specific surface marker ASGR1 (Figure S4J). Fifth, this differentiation approach yielded significantly higher expression of hepatocyte markers (Figures S5A–S5C), including ALBUMIN, AAT, and CPS1 within 18 days when compared with other methods (Si-Tayeb et al., 2010; Zhao et al., 2013) at the same time point (Figure 5A), as revealed by wide-field imaging of entire wells of differentiated cells (Figure 5B).

Given that previous differentiation protocols yielded hPSC-derived hepatocyte-like cells also displaying some extent of *in vitro* functionality (Espejel et al., 2010; Ogawa et al., 2013; Rashid et al., 2010; Si-Tayeb et al., 2010; Takebe et al., 2013; Zhao et al., 2013), we focused next on expression of tyrosine metabolic pathway enzymes including FAH (Figures S4A–S4G). Tyrosine metabolism is an important function executed by hepatocytes, and expression of tyrosine metabolic enzymes in hPSC-derived hepatocytes is pertinent to the treatment of the FRG mouse model of hereditary tyrosinemia (described later).

To track the expression of FAH at a single-cell level in hPSC-derived hepatocytes, we used CRISPR/Cas9-mediated gene editing to generate a *FAH-2A-Clover* knockin H1 hESC reporter line in which the *FAH* coding sequence was left intact (Figures 5C, 5D, and S5D–S5J). Applying the aforementioned differentiation protocol to *FAH-2A-Clover* hESCs revealed that $81.5 \pm 3.2\%$ of day-18 hepatocyte-like cells were FAH-Clover⁺ (Figure 5E). Attesting to the faithfulness of the reporter, FACS (fluorescence-activated cell sorting)-sorted Clover⁺ day-18 cells were significantly enriched for *FAH*, *ALBUMIN*, and *HGD* mRNAs by comparison to Clover⁻ cells (Figure 5F). The expression of FAH in the majority of hPSC-derived day-18 hepatocyte-like cells motivated us to test whether these populations could be used to treat the FRG mouse model of liver injury.

hPSC-Derived Hepatocytes Engraft the Injured Mouse Liver and Improve Survival during Liver Injury

Finally, we tested whether FAH⁺ day-18 hPSC-derived hepatocyte-like cells derived using our differentiation schema could engraft injured FRG mice. FRG mice are an immunodeficient mouse model of tyrosinemia type I, an inherited liver failure syndrome caused by *FAH* mutations in patients (Labelle et al., 1993; St-Louis and Tanguay, 1997). Like human patients, FRG mice suffer chronic and, eventually, fatal liver injury in the absence of a hepatoprotective drug, NTBC (Azuma et al., 2007; Overturf et al., 1996).

To this end, day-18 hPSC-derived hepatocytes were doubly labeled with constitutively expressed genetic reporters (*EF1A-BCL2-2A-GFP* and *UBC-tdTomato-2A-Luciferase*; Loh et al., 2016) and then were intrahepatically injected into neonatal FRG mice (less than 2 days old). Injected mice were allowed to grow until 6 weeks of age before liver injury was induced by cyclical withdrawal of hepatoprotective drug NTBC (Figure S6A) (Azuma et al., 2007; Overturf et al., 1996; Zhu et al., 2014) (Figure 6A). Strikingly, hPSC-derived hepatocytes engrafted in 7 out of 15 mice (Figure 6B) and continued to expand *in vivo* as shown by an increase in bioluminescence intensity over time (Figures 6B, S6B, and S6E). After ~10 weeks of liver injury, all surviving mice had detectable bioluminescence (indicating the presence of transplanted cells); mice that initially had little/no

bioluminescence had died by this time point (Figure 6B). This suggests that engrafted hPSC-derived hepatocytes promoted the survival of the FRG mice. In mice that survived 5 months post-transplantation, human ALBUMIN⁺ tdTomato⁺ liver cells resided near the liver vasculature (Figures S6C and S6D).

We further tested the ability of day-18 hPSC-derived hepatocytes to ameliorate liver failure in a second mouse model by intrasplenically transplanting them into 4- to 6-week-old adult FRG mice (Figure S6E) and inducing chronic liver injury by intermittent NTBC withdrawal (Figure 6A). Primary adult human hepatocytes were transplanted as positive controls. 72.7% of the FRG mice transplanted with hPSC-derived hepatocytes survived longer, compared to negative control mice that were not injected with any cells (Figures 6C and S6F). 1 month post-transplantation of hPSC-derived hepatocyte-like cells, human ALBUMIN⁺ liver cells were detected in the mouse liver, some of which were localized near the vasculature (Figure 6D). Mice transplanted with either hPSC-derived hepatocyte-like cells (n = 7 mice) or primary human hepatocytes (n = 5 mice) had, on average, 120 ± 36 ng/mL and 2.06 µg/mL of human ALBUMIN protein in mouse bloodstream 1 month post-transplantation (Figure 6E). This indicated that engrafted hPSC-derived hepatocytes secreted ALBUMIN into the bloodstream, albeit ~18-fold less than human adult hepatocytes (Figure 6E). Finally, bilirubin levels (reflecting the extent of liver injury) were reduced in the serum of mice transplanted with hPSC-derived or primary human hepatocytes (Figure 6F). Together, these results indicated that transplanted hPSC-derived hepatocytes engrafted the injured adult mice liver; secreted human ALBUMIN protein into the bloodstream; and most importantly, improved short-term survival in the FRG mouse model of hereditary tyrosinemia. Ultimately, this demonstrates that hPSC-derived hepatocyte-like cells are functional to some extent, in turn validating the signaling code used for their production.

Discussion

A Roadmap for Efficient Human Liver Differentiation and Blockade of Non-liver Fates

How do stem cells and progenitors exclusively commit to a single lineage amidst multiple fate options? Here, we have explored the signaling logic underlying how closely related lineages, including liver, pancreas, and intestines, arise from a common endodermal origin. Previous pathfinding PSC-to-liver differentiation studies focused solely on liver differentiation and mostly used prolonged BMP and FGF to induce liver from endoderm (Gouon-Evans et al., 2006; Shiraki et al., 2008; Si-Tayeb et al., 2010; Spence et al., 2011b; Touboul et al., 2010; Zhao et al., 2013). However, multiple endodermal lineages share a common requirement for BMP or FGF (Bhushan et al., 2001; Chung et al., 2008; Jung et al., 1999; Rossi et al., 2001; Shin et al., 2007); hence, it was unclear how these related endodermal lineages were distinguished from one another. Here, we demonstrate that mapping the parallel formation of multiple endodermal lineages provides insight into liver commitment and powerfully enables the rational suppression of unwanted, non-liver lineages during hPSC differentiation.

Our provisional roadmap for human liver development from PSCs (Figure 7) delineates a signaling code for liver development significantly extending beyond the use of prolonged BMP and FGF and illuminates several key features. First, it clarifies how hepatocyte

commitment is accomplished in stepwise fashion through signals that exclude alternate fate options (i.e., intestines, pancreas, and cholangiocytes) across different lineage branchpoints. Second, it reveals that extracellular signals act in a temporally dynamic fashion, being re-interpreted within 24 hr to exert diametrically opposing effects on liver commitment. Third, it encompasses lineage-specific surface markers useful in tracking successive steps of hepatocyte commitment. This roadmap enables one to logically and dynamically manipulate extracellular signals to systematically restrict the formation of non-liver cell types. Consequently, it is possible to rapidly and efficiently generate hPSC-derived liver bud progenitors and hepatocyte-like cells, the latter of which can engraft *in vivo* and improve the survival of injured FRG mice. Our work relied on three fundamental principles to guide liver differentiation at the expense of other lineages.

Signals Inducing Liver versus Non-liver Fates

First, we determined the signals that specify liver fate and suppress unwanted, non-liver lineage(s) at each lineage branchpoint, thus revealing how alternate fate choices are suppressed in stepwise fashion at successive stages of hepatocyte commitment. This roadmap revealed that RA initially blocks intestinal fate during posterior foregut commitment; then BMP suppresses pancreatic fate during liver commitment; finally, dual TGF- β and NOTCH blockade extinguish cholangiocyte potential during hepatocyte commitment (Figure 7).

With this knowledge, these lineage segregations could be efficiently negotiated by providing the relevant *inductive* signal(s) to drive differentiation toward the desired lineage while *repressing* the signal(s) that otherwise promoted the alternate fate (Loh et al., 2014). For example, at the pancreas-liver branchpoint, application of BMP (among other signals) specified liver bud precursors while inhibiting pancreatic fate, thus generating $94.1 \pm 7.35\%$ TBX3⁺HNF4A⁺ human liver bud progenitors by day 6 of hPSC differentiation. Later, NOTCH and TGF- β specified cholangiocytes, and thus, NOTCH and brief TGF- β inhibition drove liver bud precursors into $81.5 \pm 3.2\%$ FAH⁺ hepatocyte-like cells by day 18. While liver progenitors and hepatocytes have reportedly been efficiently generated from hPSCs (Avior et al., 2015; Carpentier et al., 2016; Ogawa et al., 2013; Si-Tayeb et al., 2010; Zhao et al., 2013), this approach to systematically block unwanted (non-liver) fates enables the accelerated derivation of liver precursors $\sim 2\text{--}3$ times faster than was previously possible and helps provide a rational framework for their efficient generation.

Temporally Dynamic Signals Controlling Foregut and Liver Specification

Second, we detailed how temporally dynamic signals specified liver fate, initially promoting but later inhibiting liver fate. For instance, over a brief 24-hr interval, RA activation and TGF- β blockade were necessary to drive definitive endoderm into posterior foregut progenitors, but 24 hr later, they limited further progression of posterior foregut toward a liver bud fate. This helped explain how multiple endodermal lineages become diversified at successive developmental steps: the same signals are re-iteratively used to accomplish different ends. This also argues against the sustained application of these (and other) signals for multiple days, which may induce extraneous, unwanted lineages. Understanding the temporal dynamics with which these signals act is critical, as these signals must be

manipulated with the same dynamism to guide efficient differentiation as cells pass through transient windows of inductive competence (Loh et al., 2014, 2016; Wang et al., 2015).

Tools for Tracking Liver Differentiation

Third, we also introduce tools to track the process of liver commitment: (1) the surface marker CD99, which, together with the absence of CD10 and CD184/CXCR4, identifies day-6 liver bud progenitors and (2) an *FAH-Clover* knockin reporter hESC line to track the subsequent generation of *FAH*⁺ hepatocyte-like cells.

Taken together, the provisional early liver developmental roadmap (Figure 7) provides a framework to understand liver commitment at the expense of non-liver fates and may avail the as-yet-unrealized goal of generating fully functional hepatocytes. Recent progress has shown that liver transcription factor overexpression can reprogram fibroblasts into more mature hepatocytes (Huang et al., 2014; Sekiya and Suzuki, 2011; Song et al., 2016; Yu et al., 2013; Zhu et al., 2014). This implies that hepatic transcription factors, when overexpressed, can engender a more mature hepatocyte state. The hPSC-derived liver progenitors generated in the present study expressed significantly higher levels of hepatic transcription factors (Figure 3) than the liver cells produced by extant differentiation methods. Thus, these liver progenitors provide a fertile venue for subsequent liver maturation efforts and, perhaps, the assembly of enhanced 3D liver “organoids” (Camp et al., 2017; Ogawa et al., 2013; Takebe et al., 2013). Indeed, the hPSC-derived hepatocyte-like day-18 cells express a repertoire of hepatocyte markers and enzymes more highly when compared with cells derived with extant protocols. A coming challenge for developmental biology at-large will be to uncover the signal(s) that mature newly born differentiated cells in the embryo into fully fledged, functional cell types in neonates and adults (Tan et al., 2017), thus extending the reach of the present roadmap.

Experimental Procedures

hPSC Differentiation and Hepatocyte Culture

mTeSR1-grown hPSCs (H1, H7, and H9 [WiCell] and ESI035 [ESI BIO]) were seeded for differentiation as single cells using Accutase (Millipore) onto Geltrex-coated plates (Thermo Fisher), at a density of 40,000 cells per well of a 12-well plate. hPSCs were differentiated into anterior primitive streak and, subsequently, into definitive endoderm by treatment with definitive endoderm Induction Medium A for 24 hr, followed by definitive endoderm Induction Medium B for 24 hr (Thermo Fisher) (Loh et al., 2014, 2016). For detailed methods, see Supplemental Information.

Data and Software Availability

The accession number for the microarray data reported in this paper is GEO: GSE98324. Imaging data are available from the Mendeley dataset: <https://doi.org/10.17632/xbtpc2pty4.1>.

Supplementary Material

Refer to Web version on PubMed Central for supplementary material.

Acknowledgments

We dedicate this paper to the memory of Professor L. Poellinger and thank him for his generous support. We thank M. Nichane, W.L. Tam, R. Ettikan, V. Luca, D. Zheng, E. Lee, D. Asraf, F. Juraimi, R. Foo, F. Michelet, W.C. Zhang, M. Boezelman, S. Vijayakumar, M.Y. Lee, B. Chua, and S.C. Ng for support and B. Wang, R. Nusse, W.C. Peng, P.A. Beachy, C.C. Khor, and H.H. Ng for discussions. This study was supported by A*STAR ETPL grant ETPL/14-R15-009 (to L.T.A. and B.L.), the Stanford-UC Berkeley Stem Cell Institute, anonymous donors, and the NIH Director's Early Independence Award DP5OD024558 (to K.M.L.).

References

- Agarwal S, Holton KL, Lanza R. Efficient differentiation of functional hepatocytes from human embryonic stem cells. *Stem Cells*. 2008; 26:1117–1127. [PubMed: 18292207]
- Avior Y, Levy G, Zimmerman M, Kitsberg D, Schwartz R, Sadeh R, Moussaieff A, Cohen M, Itskovitz-Eldor J, Nahmias Y. Microbial-derived lithocholic acid and vitamin K2 drive the metabolic maturation of pluripotent stem cells-derived and fetal hepatocytes. *Hepatology*. 2015; 62:265–278. [PubMed: 25808545]
- Azuma H, Paulk N, Ranade A, Dorrell C, Al-Dhalimy M, Ellis E, Strom S, Kay MA, Finegold M, Grompe M. Robust expansion of human hepatocytes in Fah^{-/-}Rag2^{-/-}Il2rg^{-/-} mice. *Nat Biotechnol*. 2007; 25:903–910. [PubMed: 17664939]
- Basma H, Soto-Gutiérrez A, Yannam GR, Liu L, Ito R, Yamamoto T, Ellis E, Carson SD, Sato S, Chen Y, et al. Differentiation and transplantation of human embryonic stem cell-derived hepatocytes. *Gastroenterology*. 2009; 136:990–999. [PubMed: 19026649]
- Bayha E, Jørgensen MC, Serup P, Grapin-Botton A. Retinoic acid signaling organizes endodermal organ specification along the entire antero-posterior axis. *PLoS One*. 2009; 4:e5845. [PubMed: 19516907]
- Bernardi M, Maggioli C, Zaccherini G. Human albumin in the management of complications of liver cirrhosis. *Crit Care*. 2012; 16:211. [PubMed: 22429536]
- Bhushan A, Itoh N, Kato S, Thiery JP, Czernichow P, Bellusci S, Scharfmann R. Fgf10 is essential for maintaining the proliferative capacity of epithelial progenitor cells during early pancreatic organogenesis. *Development*. 2001; 128:5109–5117. [PubMed: 11748146]
- Cai J, Zhao Y, Liu Y, Ye F, Song Z, Qin H, Meng S, Chen Y, Zhou R, Song X, et al. Directed differentiation of human embryonic stem cells into functional hepatic cells. *Hepatology*. 2007; 45:1229–1239. [PubMed: 17464996]
- Camp JG, Sekine K, Gerber T, Loeffler-Wirth H, Binder H, Gac M, Kanton S, Kageyama J, Damm G, Seehofer D, et al. Multilineage communication regulates human liver bud development from pluripotency. *Nature*. 2017; 546:533–538. [PubMed: 28614297]
- Carpentier A, Tesfaye A, Chu V, Nimgaonkar I, Zhang F, Lee SB, Thorgeirsson SS, Feinstone SM, Liang TJ. Engrafted human stem cell-derived hepatocytes establish an infectious HCV murine model. *J Clin Invest*. 2014; 124:4953–4964. [PubMed: 25295540]
- Carpentier A, Nimgaonkar I, Chu V, Xia Y, Hu Z, Liang TJ. Hepatic differentiation of human pluripotent stem cells in miniaturized format suitable for high-throughput screen. *Stem Cell Res (Amst)*. 2016; 16:640–650.
- Cascio S, Zaret KS. Hepatocyte differentiation initiates during endodermal-mesenchymal interactions prior to liver formation. *Development*. 1991; 113:217–225. [PubMed: 1764997]
- Chen YR, Sekine K, Nakamura K, Yanai H, Tanaka M, Miyajima A. Y-box binding protein-1 down-regulates expression of carbamoyl phosphate synthetase-I by suppressing CCAAT enhancer-binding protein- α function in mice. *Gastroenterology*. 2009; 137:330–340. [PubMed: 19272383]

- Chen YF, Tseng CY, Wang HW, Kuo HC, Yang VW, Lee OK. Rapid generation of mature hepatocyte-like cells from human induced pluripotent stem cells by an efficient three-step protocol. *Hepatology*. 2012; 55:1193–1203. [PubMed: 22095466]
- Chung WS, Shin CH, Stainier DYR. Bmp2 signaling regulates the hepatic versus pancreatic fate decision. *Dev Cell*. 2008; 15:738–748. [PubMed: 19000838]
- Colnot, S., Perret, C. Liver zonation In *Molecular Pathology of Liver Diseases*. Monga, SSP., editor. Boston, MA: Springer; 2011. p. 7-16.
- D'Amour KA, Agulnick AD, Eliazer S, Kelly OG, Kroon E, Baetge EE. Efficient differentiation of human embryonic stem cells to definitive endoderm. *Nat Biotechnol*. 2005; 23:1534–1541. [PubMed: 16258519]
- Duncan SA. Mechanisms controlling early development of the liver. *Mech Dev*. 2003; 120:19–33. [PubMed: 12490293]
- Espejel S, Roll GR, McLaughlin KJ, Lee AY, Zhang JY, Laird DJ, Okita K, Yamanaka S, Willenbring H. Induced pluripotent stem cell-derived hepatocytes have the functional and proliferative capabilities needed for liver regeneration in mice. *J Clin Invest*. 2010; 120:3120–3126. [PubMed: 20739754]
- Fukuda-Taira S. Hepatic induction in the avian embryo: specificity of reactive endoderm and inductive mesoderm. *J Embryol Exp Morphol*. 1981; 63:111–125. [PubMed: 7310284]
- Gordillo M, Evans T, Gouon-Evans V. Orchestrating liver development. *Development*. 2015; 142:2094–2108. [PubMed: 26081571]
- Gouon-Evans V, Boussemart L, Gadue P, Nierhoff D, Koehler CI, Kubo A, Shafritz DA, Keller G. BMP-4 is required for hepatic specification of mouse embryonic stem cell-derived definitive endoderm. *Nat Biotechnol*. 2006; 24:1402–1411. [PubMed: 17086172]
- Graf T, Enver T. Forcing cells to change lineages. *Nature*. 2009; 462:587–594. [PubMed: 19956253]
- Grapin-Botton A. Antero-posterior patterning of the vertebrate digestive tract: 40 years after Nicole Le Douarin's PhD thesis. *Int J Dev Biol*. 2005; 49:335–347. [PubMed: 15906249]
- Gualdi R, Bossard P, Zheng M, Hamada Y, Coleman JR, Zaret KS. Hepatic specification of the gut endoderm in vitro: cell signaling and transcriptional control. *Genes Dev*. 1996; 10:1670–1682. [PubMed: 8682297]
- Han S, Bourdon A, Hamou W, Dziedzic N, Goldman O, Gouon-Evans V. Generation of functional hepatic cells from pluripotent stem cells. *J Stem Cell Res Ther*. 2012; (8,Suppl 10):1–7.
- Haridass D, Yuan Q, Becker PD, Cantz T, Iken M, Rothe M, Narain N, Bock M, Nörder M, Legrand N, et al. Repopulation efficiencies of adult hepatocytes, fetal liver progenitor cells, and embryonic stem cell-derived hepatic cells in albumin-promoter-enhancer urokinase-type plasminogen activator mice. *Am J Pathol*. 2009; 175:1483–1492. [PubMed: 19717639]
- Hay DC, Zhao D, Fletcher J, Hewitt ZA, McLean D, Urruticoechea-Uriguen A, Black JR, Elcombe C, Ross JA, Wolf R, Cui W. Efficient differentiation of hepatocytes from human embryonic stem cells exhibiting markers recapitulating liver development in vivo. *Stem Cells*. 2008; 26:894–902. [PubMed: 18238852]
- Huang P, Zhang L, Gao Y, He Z, Yao D, Wu Z, Cen J, Chen X, Liu C, Hu Y, et al. Direct reprogramming of human fibroblasts to functional and expandable hepatocytes. *Cell Stem Cell*. 2014; 14:370–384. [PubMed: 24582927]
- Jacquemin P, Lemaigre FP, Rousseau GG. The Onecut transcription factor HNF-6 (OC-1) is required for timely specification of the pancreas and acts upstream of Pdx-1 in the specification cascade. *Dev Biol*. 2003; 258:105–116. [PubMed: 12781686]
- Jung J, Zheng M, Goldfarb M, Zaret KS. Initiation of mammalian liver development from endoderm by fibroblast growth factors. *Science*. 1999; 284:1998–2003. [PubMed: 10373120]
- Jungermann K. Zonation of metabolism and gene expression in liver. *Histochem Cell Biol*. 1995; 103:81–91. [PubMed: 7634156]
- Labelle Y, Phaneuf D, Leclerc B, Tanguay RM. Characterization of the human fumarylacetoacetate hydrolase gene and identification of a missense mutation abolishing enzymatic activity. *Hum Mol Genet*. 1993; 2:941–946. [PubMed: 8364576]
- Lawson KA, Meneses JJ, Pedersen RA. Clonal analysis of epiblast fate during germ layer formation in the mouse embryo. *Development*. 1991; 113:891–911. [PubMed: 1821858]

- Ledouarin N. Induction of prehepatic endoderm by mesoderm of the cardiac region in the chick embryo. *J Embryol Exp Morphol.* 1964; 12:651–664. [PubMed: 14251477]
- Lemaigre FP. Mechanisms of liver development: concepts for understanding liver disorders and design of novel therapies. *Gastroenterology.* 2009; 137:62–79. [PubMed: 19328801]
- Lewis SL, Tam PPL. Definitive endoderm of the mouse embryo: formation, cell fates, and morphogenetic function. *Dev Dyn.* 2006; 235:2315–2329. [PubMed: 16752393]
- Loh KM, Ang LT, Zhang J, Kumar V, Ang J, Auyeong JQ, Lee KL, Choo SH, Lim CY, Nichane M, et al. Efficient endoderm induction from human pluripotent stem cells by logically directing signals controlling lineage bifurcations. *Cell Stem Cell.* 2014; 14:237–252. [PubMed: 24412311]
- Loh KM, Chen A, Koh PW, Deng TZ, Sinha R, Tsai JM, Barkal AA, Shen KY, Jain R, Morganti RM, et al. Mapping the pairwise choices leading from pluripotency to human bone, heart, and other mesoderm cell types. *Cell.* 2016; 166:451–467. [PubMed: 27419872]
- Lokmane L, Haumaitre C, Garcia-Villalba P, Anselme I, Schneider-Maunoury S, Cereghini S. Crucial role of vHNF1 in vertebrate hepatic specification. *Development.* 2008; 135:2777–2786. [PubMed: 18635606]
- Lüdtke THW, Christoffels VM, Petry M, Kispert A. Tbx3 promotes liver bud expansion during mouse development by suppression of cholangiocyte differentiation. *Hepatology.* 2009; 49:969–978. [PubMed: 19140222]
- McCracken KW, Catá EM, Crawford CM, Sinagoga KL, Schumacher M, Rockich BE, Tsai YH, Mayhew CN, Spence JR, Zavros Y, Wells JM. Modelling human development and disease in pluripotent stem-cell-derived gastric organoids. *Nature.* 2014; 516:400–404. [PubMed: 25363776]
- McLin VA, Rankin SA, Zorn AM. Repression of Wnt/beta-catenin signaling in the anterior endoderm is essential for liver and pancreas development. *Development.* 2007; 134:2207–2217. [PubMed: 17507400]
- Miyajima A, Tanaka M, Itoh T. Stem/progenitor cells in liver development, homeostasis, regeneration, and reprogramming. *Cell Stem Cell.* 2014; 14:561–574. [PubMed: 24792114]
- Nissim S, Sherwood RI, Wucherpennig J, Saunders D, Harris JM, Esain V, Carroll KJ, Frechette GM, Kim AJ, Hwang KL, et al. Prostaglandin E2 regulates liver versus pancreas cell-fate decisions and endodermal outgrowth. *Dev Cell.* 2014; 28:423–437. [PubMed: 24530296]
- Ogawa S, Surapitsitach J, Virtanen C, Ogawa M, Niapour M, Sugamori KS, Wang S, Tamblyn L, Guillemette C, Hoffmann E, et al. Three-dimensional culture and cAMP signaling promote the maturation of human pluripotent stem cell-derived hepatocytes. *Development.* 2013; 140:3285–3296. [PubMed: 23861064]
- Ogawa M, Ogawa S, Bear CE, Ahmadi S, Chin S, Li B, Grompe M, Keller G, Kamath BM, Ghanekar A. Directed differentiation of cholangiocytes from human pluripotent stem cells. *Nat Biotechnol.* 2015; 33:853–861. [PubMed: 26167630]
- Overturf K, Al-Dhalimy M, Tanguay R, Brantly M, Ou CN, Finegold M, Grompe M. Hepatocytes corrected by gene therapy are selected in vivo in a murine model of hereditary tyrosinaemia type I. *Nat Genet.* 1996; 12:266–273. [PubMed: 8589717]
- Rankin SA, Kormish J, Kofron M, Jegga A, Zorn AM. A gene regulatory network controlling *hhx* transcription in the anterior endoderm of the organizer. *Dev Biol.* 2011; 351:297–310. [PubMed: 21215263]
- Rashid ST, Corbineau S, Hannan N, Marciniak SJ, Miranda E, Alexander G, Huang-Doran I, Griffin J, Ahrlund-Richter L, Skepper J, et al. Modeling inherited metabolic disorders of the liver using human induced pluripotent stem cells. *J Clin Invest.* 2010; 120:3127–3136. [PubMed: 20739751]
- Rossi JM, Dunn NR, Hogan BL, Zaret KS. Distinct meso-dermal signals, including BMPs from the septum transversum mesenchyme, are required in combination for hepatogenesis from the endoderm. *Genes Dev.* 2001; 15:1998–2009. [PubMed: 11485993]
- Rostovskaya M, Bredenkamp N, Smith A. Towards consistent generation of pancreatic lineage progenitors from human pluripotent stem cells. *Philos Trans R Soc Lond B Biol Sci.* 2015; 370:20140365. [PubMed: 26416676]
- Sampaziotis F, de Brito MC, Madrigal P, Bertero A, Saeb-Parsy K, Soares FAC, Schrupf E, Melum E, Karlsen TH, Bradley JA, et al. Cholangiocytes derived from human induced pluripotent stem

- cells for disease modeling and drug validation. *Nat Biotechnol.* 2015; 33:845–852. [PubMed: 26167629]
- Sekine S, Lan BYA, Bedolli M, Feng S, Hebrok M. Liver-specific loss of β -catenin blocks glutamine synthesis pathway activity and cytochrome p450 expression in mice. *Hepatology.* 2006; 43:817–825. [PubMed: 16557553]
- Sekiya S, Suzuki A. Direct conversion of mouse fibroblasts to hepatocyte-like cells by defined factors. *Nature.* 2011; 475:390–393. [PubMed: 21716291]
- Serls AE, Doherty S, Parvatiyar P, Wells JM, Deutsch GH. Different thresholds of fibroblast growth factors pattern the ventral foregut into liver and lung. *Development.* 2005; 132:35–47. [PubMed: 15576401]
- Sherwood RI, Maehr R, Mazzoni EO, Melton DA. Wnt signaling specifies and patterns intestinal endoderm. *Mech Dev.* 2011; 128:387–400. [PubMed: 21854845]
- Shin D, Shin CH, Tucker J, Ober EA, Rentzsch F, Poss KD, Hammerschmidt M, Mullins MC, Stainier DYR. Bmp and Fgf signaling are essential for liver specification in zebrafish. *Development.* 2007; 134:2041–2050. [PubMed: 17507405]
- Shiojiri N, Wada JI, Tanaka T, Noguchi M, Ito M, Gebhardt R. Heterogeneous hepatocellular expression of glutamine synthetase in developing mouse liver and in testicular transplants of fetal liver. *Lab Invest.* 1995; 72:740–747. [PubMed: 7783431]
- Shiojiri N, Takeshita K, Yamasaki H, Iwata T. Suppression of C/EBP α expression in biliary cell differentiation from hepatoblasts during mouse liver development. *J Hepatol.* 2004; 41:790–798. [PubMed: 15519652]
- Shiraki N, Umeda K, Sakashita N, Takeya M, Kume K, Kume S. Differentiation of mouse and human embryonic stem cells into hepatic lineages. *Genes Cells.* 2008; 13:731–746. [PubMed: 18513331]
- Si-Tayeb K, Noto FK, Nagaoka M, Li J, Battle MA, Duris C, North PE, Dalton S, Duncan SA. Highly efficient generation of human hepatocyte-like cells from induced pluripotent stem cells. *Hepatology.* 2010; 51:297–305. [PubMed: 19998274]
- Smith DD Jr, Campbell JW. Distribution of glutamine synthetase and carbamoyl-phosphate synthetase I in vertebrate liver. *Proc Natl Acad Sci USA.* 1988; 85:160–164. [PubMed: 2893372]
- Song Z, Cai J, Liu Y, Zhao D, Yong J, Duo S, Song X, Guo Y, Zhao Y, Qin H, et al. Efficient generation of hepatocyte-like cells from human induced pluripotent stem cells. *Cell Res.* 2009; 19:1233–1242. [PubMed: 19736565]
- Song G, Pacher M, Balakrishnan A, Yuan Q, Tsay HC, Yang D, Reetz J, Brandes S, Dai Z, Pützer BM, et al. Direct reprogramming of hepatic myofibroblasts into hepatocytes in vivo attenuates liver fibrosis. *Cell Stem Cell.* 2016; 18:797–808. [PubMed: 26923201]
- Spence JR, Lange AW, Lin SCJ, Kaestner KH, Lowy AM, Kim I, Whitsett JA, Wells JM. Sox17 regulates organ lineage segregation of ventral foregut progenitor cells. *Dev Cell.* 2009; 17:62–74. [PubMed: 19619492]
- Spence JR, Lauf R, Shroyer NF. Vertebrate intestinal endoderm development. *Dev Dyn.* 2011a; 240:501–520. [PubMed: 21246663]
- Spence JR, Mayhew CN, Rankin SA, Kuhar MF, Vallance JE, Tolle K, Hoskins EE, Kalinichenko VV, Wells SI, Zorn AM, et al. Directed differentiation of human pluripotent stem cells into intestinal tissue in vitro. *Nature.* 2011b; 470:105–109. [PubMed: 21151107]
- Spijkers JA, van den Hoff MJ, Hakvoort TB, Vermeulen JL, Tesink-Taekema S, Lamers WH. Foetal rise in hepatic enzymes follows decline in c-met and hepatocyte growth factor expression. *J Hepatol.* 2001; 34:699–710. [PubMed: 11434616]
- St-Louis M, Tanguay RM. Mutations in the fumarylacetoacetate hydrolase gene causing hereditary tyrosinemia type I: overview. *Hum Mutat.* 1997; 9:291–299. [PubMed: 9101289]
- Stafford D, Prince VE. Retinoic acid signaling is required for a critical early step in zebrafish pancreatic development. *Curr Biol.* 2002; 12:1215–1220. [PubMed: 12176331]
- Suzuki A, Sekiya S, Büscher D, Izpisua Belmonte JC, Taniguchi H. Tbx3 controls the fate of hepatic progenitor cells in liver development by suppressing p19ARF expression. *Development.* 2008a; 135:1589–1595. [PubMed: 18356246]

- Suzuki A, Sekiya S, Onishi M, Oshima N, Kiyonari H, Nakauchi H, Taniguchi H. Flow cytometric isolation and clonal identification of self-renewing bipotent hepatic progenitor cells in adult mouse liver. *Hepatology*. 2008b; 48:1964–1978. [PubMed: 18837044]
- Takebe T, Sekine K, Enomura M, Koike H, Kimura M, Ogaeri T, Zhang RR, Ueno Y, Zheng YW, Koike N, et al. Vascularized and functional human liver from an iPSC-derived organ bud transplant. *Nature*. 2013; 499:481–484. [PubMed: 23823721]
- Tam PP, Beddington RS. The formation of mesodermal tissues in the mouse embryo during gastrulation and early organogenesis. *Development*. 1987; 99:109–126. [PubMed: 3652985]
- Tan AKY, Loh KM, Ang LT. Evaluating the regenerative potential and functionality of human liver cells in mice. *Differentiation*. 2017; 98:25–34. [PubMed: 29078082]
- Tennent GA, Brennan SO, Stangou AJ, O'Grady J, Hawkins PN, Pepys MB. Human plasma fibrinogen is synthesized in the liver. *Blood*. 2007; 109:1971–1974. [PubMed: 17082318]
- Thomas PQ, Brown A, Beddington RS. Hex: a homeobox gene revealing peri-implantation asymmetry in the mouse embryo and an early transient marker of endothelial cell precursors. *Development*. 1998; 125:85–94. [PubMed: 9389666]
- Tiso N, Filippi A, Pauls S, Bortolussi M, Argenton F. BMP signalling regulates anteroposterior endoderm patterning in zebrafish. *Mech Dev*. 2002; 118:29–37. [PubMed: 12351167]
- Touboul T, Hannan NR, Corbineau S, Martinez A, Martinet C, Branchereau S, Mainot S, Strick-Marchand H, Pedersen R, Di Santo J, et al. Generation of functional hepatocytes from human embryonic stem cells under chemically defined conditions that recapitulate liver development. *Hepatology*. 2010; 51:1754–1765. [PubMed: 20301097]
- Tremblay KD, Zaret KS. Distinct populations of endoderm cells converge to generate the embryonic liver bud and ventral foregut tissues. *Dev Biol*. 2005; 280:87–99. [PubMed: 15766750]
- Wandzioch E, Zaret KS. Dynamic signaling network for the specification of embryonic pancreas and liver progenitors. *Science*. 2009; 324:1707–1710. [PubMed: 19556507]
- Wang A, Yue F, Li Y, Xie R, Harper T, Patel NA, Muth K, Palmer J, Qiu Y, Wang J, et al. Epigenetic priming of enhancers predicts developmental competence of hESC-derived endodermal lineage intermediates. *Cell Stem Cell*. 2015; 16:386–399. [PubMed: 25842977]
- Yu B, He ZY, You P, Han QW, Xiang D, Chen F, Wang MJ, Liu CC, Lin XW, Borjigin U, et al. Reprogramming fibroblasts into bipotential hepatic stem cells by defined factors. *Cell Stem Cell*. 2013; 13:328–340. [PubMed: 23871605]
- Zhao D, Chen S, Duo S, Xiang C, Jia J, Guo M, Lai W, Lu S, Deng H. Promotion of the efficient metabolic maturation of human pluripotent stem cell-derived hepatocytes by correcting specification defects. *Cell Res*. 2013; 23:157–161. [PubMed: 23070301]
- Zhu S, Rezvani M, Harbell J, Mattis AN, Wolfe AR, Benet LZ, Willenbring H, Ding S. Mouse liver repopulation with hepatocytes generated from human fibroblasts. *Nature*. 2014; 508:93–97. [PubMed: 24572354]
- Zorn AM, Wells JM. Vertebrate endoderm development and organ formation. *Annu Rev Cell Dev Biol*. 2009; 25:221–251. [PubMed: 19575677]

Highlights

- A roadmap for efficient human liver development and blockade of non-liver fates
- Dynamic signals induced or repressed liver formation in a 24-hr interval
- Stage-specific diagnostic surface markers tracking human liver differentiation
- hPSC-derived hepatocytes improved short-term survival of injured *Fah*^{-/-} mice

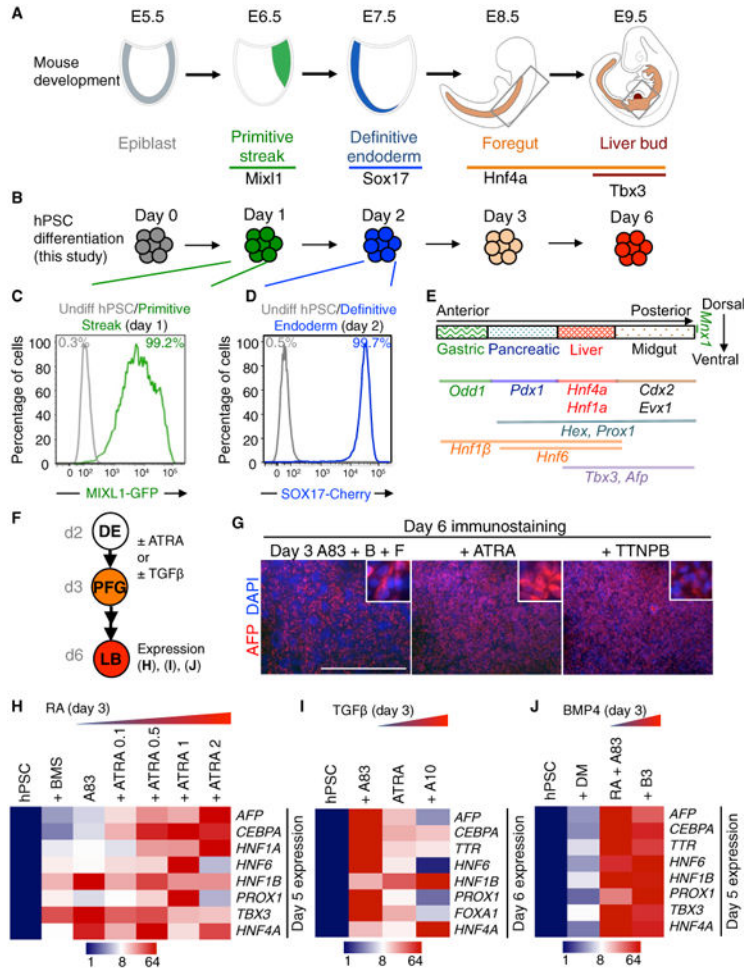


Figure 1. Differentiation of Human Definitive Endoderm into Posterior Foregut
 (A) Liver development in the mouse embryo between E5.5 to E9.5 depicting *Mixl1*⁺ primitive streak, *Sox17*⁺ definitive endoderm, *Hnf4a*⁺ foregut, and *Tbx3*⁺ liver bud progenitors.
 (B) Overview of human PSC differentiation strategy in this study.
 (C) Percentage of *MIXL1-GFP*⁺ cells using *MIXL1-GFP* knockin hESC reporter line (Loh et al., 2014).
 (D) Percentage of *SOX17-mCherry*⁺ cells using *SOX17-mCherry* knockin hESC reporter line (Loh et al., 2014).
 (E) Markers expressed in E9.5 mouse liver bud progenitors.
 (F) Strategy to treat definitive endoderm (DE) with RA or TGF- β modulators on the day-2 to day-3 interval to produce day-3 posterior foregut (PFG) and assaying subsequent effects on liver bud gene expression by day 6, as shown in (H)–(J).
 (G) Transient treatment on the day-2 to day-3 interval with ATRA or TTNPB markedly improves AFP expression in day-6 hPSC-derived liver bud progenitors on top of base media condition A83 + B + F (A83 + B + F: A8301, 1 μ M; BMP4, 30 ng/mL; FGF2, 10 ng/mL), as shown by immunostaining with a DAPI nuclear counterstain. Scale bar, 1 mm.

(H) qPCR gene expression of day-5 liver bud cells generated from endoderm cells briefly treated on the day-2 to day-3 interval with a retinoid inhibitor (BMS: BMS493, 10 μ M) or ATRA of varying doses (0.1 mM, 0.5 μ M, 1 μ M, or 2 μ M) on top of base media condition A83 (A83: A8301, 1 μ M).

(I) qPCR gene expression of day-6 liver bud cells generated from endoderm cells briefly treated on the day-2 to day-3 interval with a TGF- β inhibitor A83 (A83: A8301, 1 μ M) or a TGF- β agonist (A10: ACTIVIN, 10 ng/mL) on top of base media condition ATRA (ATRA: 2 μ M).

(J) qPCR gene expression of day-5 liver bud cells generated from endoderm cells briefly treated on the day-2 to day-3 interval with a BMP inhibitor DM (DM: DM3189, 250 nM) or a BMP agonist (B3: BMP4, 3 ng/mL) on top of base media condition RA + A83 (RA: ATRA, 2 μ M; A83: A8301, 1 μ M).

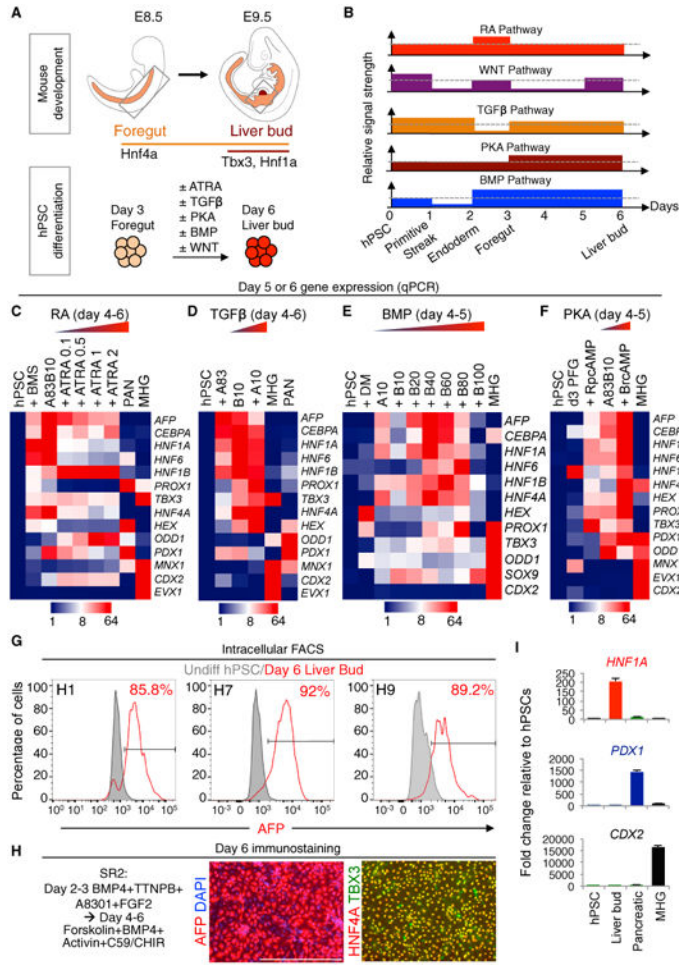


Figure 2. Accelerated Generation of Human TBX3⁺HNF4A⁺AFP⁺ Liver Bud Progenitors by Day 6 of hPSC Differentiation

(A) Development of liver bud in mouse embryos. Strategy to treat posterior foregut with RA, TGF-β, PKA, BMP, and WNT modulators on the day-4 to day-6 interval to produce day-6 liver bud progenitors and assaying effects on liver bud gene expression by day 6, as shown in (C)–(F).

(B) Temporally dynamic signals govern liver differentiation.

(C) qPCR gene expression of day-6 liver bud cells generated from endoderm treated on the day-4 to day-6 interval with a retinoid inhibitor (BMS: BMS493, 10 μM) or varying doses of a retinoid agonist (ATRA, 0.1 μM, 0.5 μM, 1 μM, and 2 μM) on top of base media condition A83B10 (A83B10: A8301, 1 μM; BMP4, 10 ng/mL) and qPCR gene expression of day-6 hPSC-derived midgut/hindgut (MHG) or pancreatic endoderm (PAN) cells.

(D) qPCR gene expression of day-6 liver bud cells generated from endoderm treated on the day-4 to day-6 interval with a TGF-β inhibitor (A83: A8301, 1 μM) or ACTIVIN (10 ng/mL) on top of base media condition B10 (B10: BMP4, 10 ng/mL). Day-6 hPSC-derived pancreatic endoderm (PAN) or midgut/hindgut cells were included as controls.

(E) qPCR gene expression of day-5 liver bud cells generated from endoderm treated on the day-4 to day-5 interval with a BMP inhibitor (DM: DM3189, 250 nM) or varying doses of

BMP4 (B, 10–100 ng/mL) in the presence of base media condition A10 (A10: ACTIVIN at 10 ng/mL). Midgut/hindgut denotes hPSC-derived midgut/hindgut cells.

(F) Gene expression of day-6 liver bud cells after 2-day treatment of PKA inhibitor (RpCAMP, 100 μ M) or PKA agonist (BrCAMP, 1 mM) in the presence of base media condition A83B10 (A83B10: A8301, 1 μ M; BMP4, 10 ng/mL) during a day-4 to day-5 interval and day-6 hPSC-derived midgut/hindgut, as shown by qPCR.

(G) Percentage of day-6 liver bud progenitors positive for AFP from the differentiation of 3 hPSC lines (H1, H7, and H9) as shown by intracellular FACS.

(H) Day-6H1hPSC-derived liver progenitors generated using SR2 were immunostained for AFP, HNF4A, and TBX3 with a DAPI nuclear counterstain. Scalebar, 500 μ m.

(I) Gene expression of day-6 liver progenitors, pancreatic endoderm, and midgut/hindgut progenitors derived from hPSCs for *HNF1A*, *PDX1*, and *CDX2*. Error bars represent \pm SE.

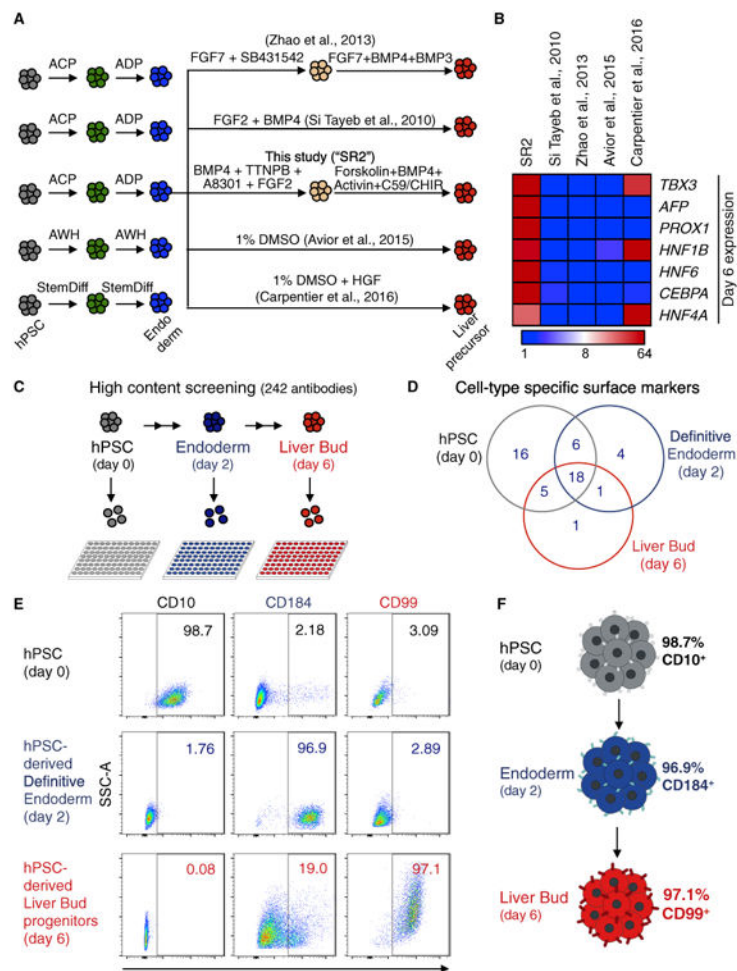


Figure 3. High-Throughput Screening Identifies Liver-Specific Surface Markers during PSC Differentiation

(A) Schematic diagram of liver differentiation approaches including SR2 and other methods (Zhao et al., 2013; Si-Tayeb et al., 2010; Avior et al., 2015; Carpentier et al., 2016).

Primitive-streak-inducing conditions: ACP, ACTIVIN + CHIR99201 + PI103 (Loh et al., 2014); AWH, ACTIVIN + Wnt3a + HGF (Avior et al., 2015); StemDiff, STEMdiff definitive endoderm differentiation kit. Endoderm-inducing condition: ADP, ACTIVIN + DM3189 + PI103 (Loh et al., 2014). Liver progenitors were analyzed at day 6 (Zhao et al., 2013; Si Tayeb et al., 2010) or day 7 (Avior et al., 2015; Carpentier et al., 2016), respectively, as described in the respective studies.

(B) qPCR gene expression of day-6H1 hPSC-derived liver progenitors generated using SR2 or other methods (Si-Tayeb et al., 2010; Zhao et al., 2013; Avior et al., 2015; Carpentier et al., 2016).

(C) Strategy to conduct high-throughput FACS screening of surface markers expressed on H7 hPSCs, day-2 H7 hPSC-derived endoderm, and day-6 H7 hPSC-derived liver bud progenitors.

(D) Venn diagram of surface markers expressed on hPSCs, day-2 hPSC-derived definitive endoderm, and day-6 hPSC-derived liver bud progenitors.

(E) hPSCs, hPSC-derived definitive endoderm, and liver bud progenitors stained for CD10, CD184, and CD99, as shown by live-cell FACS.

(F) Surface markers expressed on hPSC and day-2 hPSC-derived definitive endoderm and day-6 liver progenitors; summary of present work.

Author Manuscript

Author Manuscript

Author Manuscript

Author Manuscript

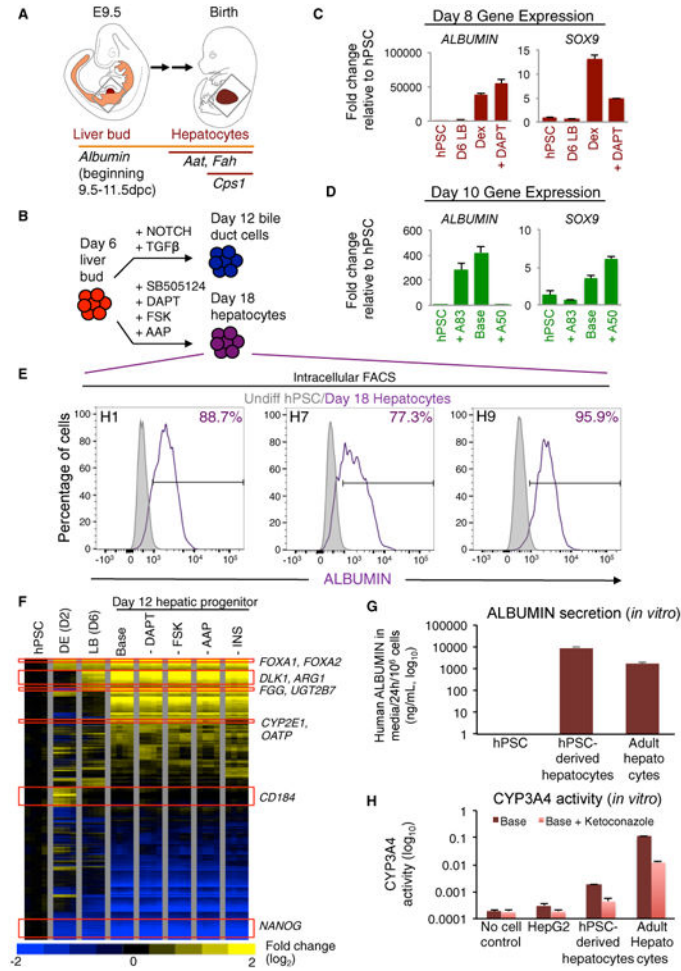


Figure 4. Generation of Enriched Populations of ALBUMIN⁺ and FAH⁺ Immature Hepatocytes by Day 18 of hPSC Differentiation

(A) Diagram depicting liver development in mouse embryos between E9.5 and birth and the expression of various liver genes. dpc, days post-coitum.

(B) A schematic of the present work showing the differentiation of human liver bud progenitors into bile duct cells or hepatocytes. A8301, TGF-β inhibitor; DAPT, Notch inhibitor; FSK, forskolin; AAP, ascorbic acid-2-phosphate.

(C and D) qPCR gene expression of day-6 hPSC-derived liver bud (LB) progenitors before and after 2-day treatment of 10 μM DAPT in the absence or presence of (C) 10 μM dexamethasone (Dex) or (D) a TGF-β inhibitor (A83: A83-01, 1 μM) or ACTIVIN (10, 30, or 50 ng/mL) on top of base media condition.

(E) ALBUMIN intracellular FACS analysis of hPSCs or day-18 hepatocytes derived from hPSC lines H1, H7, and H9.

(F) Global microarray gene expression of hPSCs, day-2 definitive endoderm, day-6 liver bud (LB) progenitors, and day-12 hPSC-derived hepatic progenitors that were either induced using the full combination (base) or with the individual omission of either DAPT, forskolin, ascorbic acid-2-phosphate, or insulin during the liver bud → hepatic progenitor differentiation step to reveal genes whose expression is regulated by DAPT, FSK, AAP, and insulin (INS). 4 biological replicates were used for the microarray analyses.

(G) ALBUMIN levels detected in culture medium grown with hPSC-derived or primary adult human hepatocytes as measured by ELISA with a human-specific ALBUMIN antibody; “Base” denotes culture medium alone.

(H) CYP3A4 activity of hPSCs, HepG2, and hPSC-derived hepatocytes (Day-18 Hep), as measured by P450-Glo luciferase assays and abolished by CYP3A4 inhibitor ketoconazole; signal is further normalized to cell number baseline, as measured by CellTiter-Glo.

Error bars represent \pm SE.

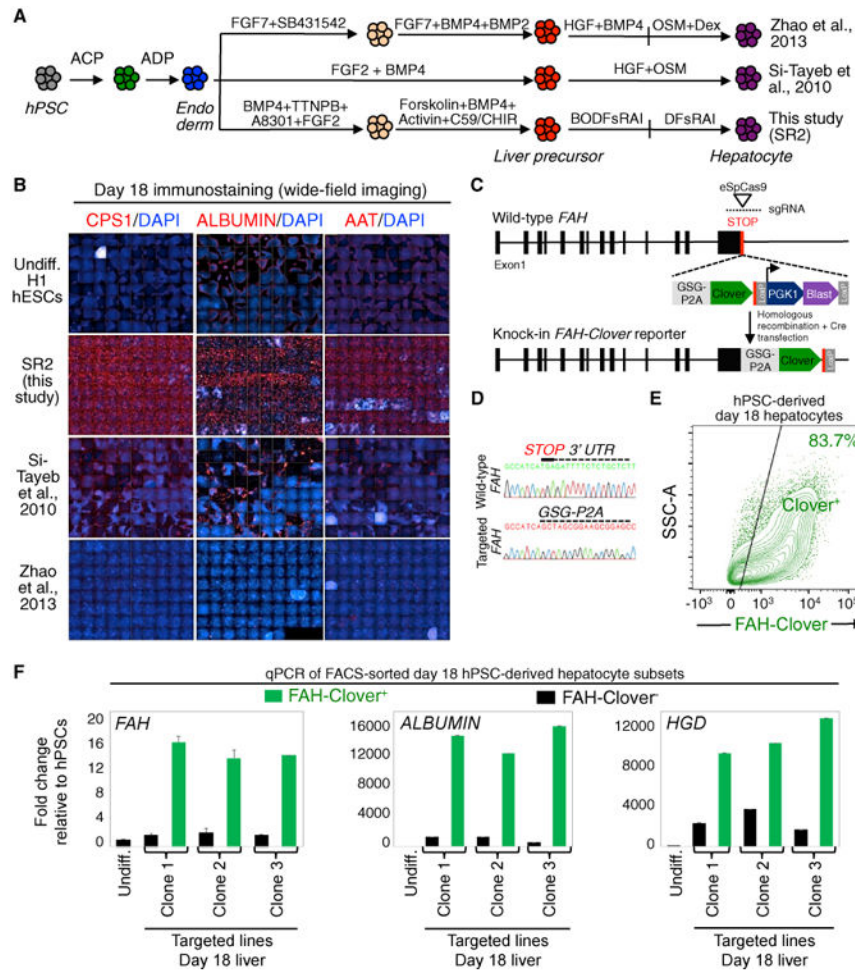


Figure 5. Generation of a *FAH*-2A-Clover Knockin H1 hPSC Reporter Line Using CRISPR/Cas9-Mediated Gene Editing

(A) Schematic diagram of liver differentiation approaches, including SR2 or other methods (Zhao et al., 2013; Si-Tayeb et al., 2010). Primitivestreak-inducing conditions: ACP, ACTIVIN + CHIR99201 + PI103 (Loh et al., 2014). Endoderm-inducing condition: ADP, ACTIVIN + DM3189 + PI103 (Loh et al., 2014). Hepatocyte-inducing condition: BODFsRAI, BMP4 + OSM + dexamethasone (Dex) + forskolin + Ro4929097 + AA2P + insulin. For detailed methods, see Supplemental Information.

(B) Day-18 hepatocyte-like cells generated by 3 methods (SR2 [the method described in the present work] or previously reported methods [Si-Tayeb et al., 2010; Zhao et al., 2013]) were immunostained for carbamoyl phosphate synthetase 1 (CPS1), ALBUMIN (ALB), and Alpha-1 anti-trypsin (AAT) with a DAPI nuclear counterstain, and multiple fields were stitched into 1 image.

(C) Schematic illustration of the strategy to insert a P2A-Clover reporter cassette into the *FAH* locus. A Gly-Ser-Gly (gsg) sequence was added to the start of the P2A sequence; eSpCas9, enhanced specificity Cas9; PGK1, Phosphoglycerate kinase 1 promoter; Blast, Blasticidin drug resistance gene.

(D) Wild-type and knockin alleles of the *FAH* locus sequenced by PCR.

(E) FACS analysis of the day-18 hPSC-derived hepatocyte-like population revealed that it was 83.7% FAH-Clover⁺.

(F) FACS-sorted FAH-Clover⁺ day-18 H1-derived hepatocyte-like cells (green bars) were significantly enriched for liver genes *FAH*, *ALBUMIN*, and *HGD* mRNAs when compared with FAH-Clover⁻ cells (black bars) as shown by qPCR. Consistent results were obtained across multiple independent *FAH-2A-Clover* knockin H1 hPSC reporter clones (#1-3). Error bars represent \pm SE.

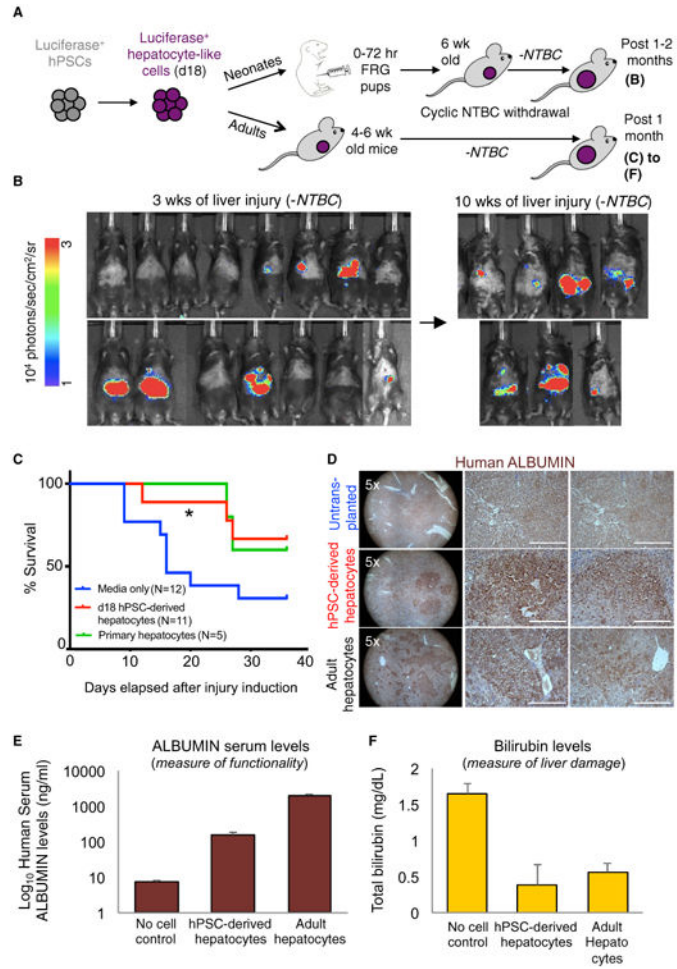


Figure 6. Human PSC-Derived Hepatocytes Engraft Neonatal and Adult *Fah*^{-/-} *Rag2*^{-/-} *Ilr2g*^{-/-} Mice and Improve Short-Term Survival

(A) Strategy to inject hPSC-derived hepatocytes into the livers of neonatal FRG mice (0–72 hr old) or adult *Fah*^{-/-} *Rag2*^{-/-} *Ilr2g*^{-/-} (FRG) mice (4–6 weeks old) and to subsequently induce liver injury; H9 *EF1A-BCL2-2A-GFP*; *UBC-tdTomato-2A-Luciferase* hPSCs (Loh et al., 2016) were used to generate hepatocytes for injections.

(B) Bioluminescent imaging of adult FRG mice that were intrahepatically injected with Luciferase⁺ day-18 hPSC-derived hepatocytes while they were neonates. Liver injury was induced at weeks 4 to 6 by withdrawing NTBC; the remaining mice at 3 or 10 weeks post-injury are shown.

(C) Adult FRG mice were injected with Luciferase⁺ day-18 hPSC-derived hepatocytes. Kaplan-Meier's survival curves depicting the percent survival (after NTBC withdrawal) of adult FRG mice that had either been injected with day-18 hPSC-derived hepatocytes (n = 11), primary adult human hepatocytes (red line; n = 5), or media-only control (blue line; n = 12); Mantel-Cox log-rank test, *p < 0.05, from 3 independent experiments.

(D) Adult FRG mice were intrasplenically injected with day-18 hPSC-derived or primary adult human hepatocytes and NTBC was withheld. One month later, engrafted livers stained positive for human ALBUMIN (brown; at 5× or 20× magnifications), as shown by immunostaining. Scale bars, 200 μm. Image is representative of 5 livers.

(E) *In vivo* secretion of human serum ALBUMIN secretion into the bloodstream *in vivo* by hPSC-derived or primary adult human hepatocytes, as measured by ELISA, 1 month post-transplant.

(F) Reduction of bilirubin levels in the serum of mice transplanted with hPSC-derived or primary adult human hepatocytes versus negative or no-cell media-only control, 1 month post-transplant.

Error bars represent \pm SE.

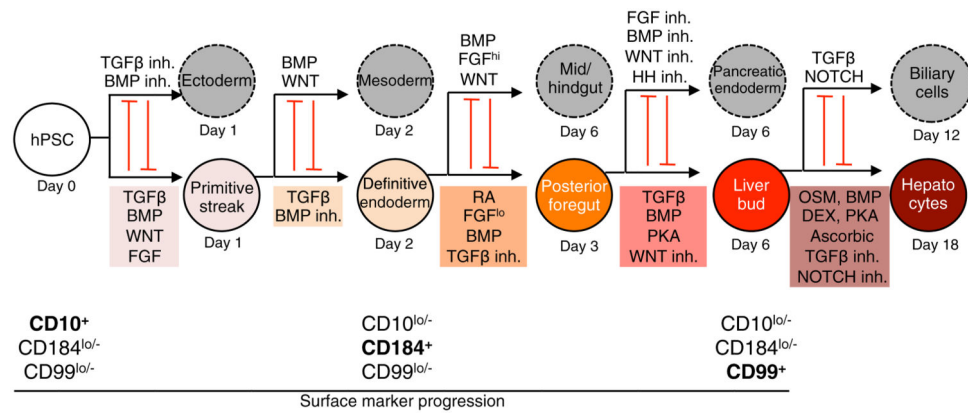


Figure 7. A Signaling Roadmap to Efficiently Generate Human Liver Cells from PSCs
 Summary of the present work. Inh., inhibitor; hi., high; lo., low; Ascorbic, ascorbic acid-2-phosphate. Optionally, Wnt inhibitor was added on days 4–5, and TGF-β inhibitor was added on days 7–8. Surface markers expressed on hPSC, day-2 hPSC-derived definitive endoderm, and day-6 liver bud progenitors are detailed in Results and Figure 3.